Journal of Mechanical and Automation Engineering

Received: Dec 08, 2015
Accepted: Dec 20, 2015
Published: Dec 23, 2015

http://dx.doi.org/10.14437/JMAE-1-103

Research

Li-Hong Juang, J Mech Auto Eng 2015, 1:1

Phase Border Removing of MRI Brain Image by Wavelet Transform with Symmetrization Technique

Li-Hong Juang[*] and Lixin Zheng

Science & Technology Innovation Center, Engineering College, HuaQiao University, Fujian, P.R. China

Abstract

We present a preliminary design and experimental results of phase discontinuity relaxation method for Magnetic Resonance Imaging (MRI) phase images that utilizes wavelet transform algorithm with symmetrization technique. The method is capable of solving ambiguity problem in MRI phase image by removing the border boundary. The key idea of wavelet transform algorithm is to solve the given MRI phase data by operating frequency domain relaxation in coarse grids and transferring the intermediate result into finer grids. In this paper we investigate the possibility of employing this approach for phase image based-MRI application. We also evaluate and compare these processed images with the original image. The application of the proposed method for unborder phase is demonstrated.

Keywords: Wavelet Transform Algorithm; MRI Phase Images; Symmetrization

[*]**Corresponding Author:** Li-Hong Juang, Science & Technology Innovation Center, Engineering College, HuaQiao University, Fujian, P.R. China; E-mail: puuan.juang@msa.hinet.net

1. Introduction

Imaging is an essential aspect of medical sciences for visualization of anatomical structures and functional or metabolic information of the human body [1]. And structural and functional imaging of human body is important for understanding the human body anatomy, physiological processes, function of organs, and behavior of whole or a part of organ under the influence of abnormal physiological conditions or a disease [2, 3]. In the last two decades radiological sciences have witnessed a revolutionary progress in medical imaging and computerized medical image processing, some important radiological tools in diagnosis and treatment evaluation and intervention of critical diseases have much significant improvement in health care. At moment, medical imaging in diagnostic radiology is evolving as a result of the significant contributions of a number of different disciplines from basic sciences, engineering, and medicine. Specially, computerized image reconstruction, processing and analysis methods have been developed for medical imaging applications. For example, the application-domain knowledge has been used in developing models for accurate analysis and interpretation.

The development of imaging instrumentation has also inspired the evolution of new computerized image reconstruction, processing and analysis methods for better understanding and interpretation of medical images. The image processing and analysis methods have been used to help physicians to make important medical decision through physician-computer interaction. Recently, intelligent or model-based quantitative image analysis approaches [4, 5] have been explored for computer-aided diagnosis to improve the sensitivity and specificity of radiological tests involving medical images. These advances have led to new complex medical imaging modalities such as X-ray CT [6], Magnetic Resonance Imaging (MRI) [7, 8], SPECT [9], PET [10] and Ultrasound [11, 12] depend heavily on computer technology for creation and display of digital images. Using the computer, multidimensional digital images of physiological structures can be processed and manipulated to visualize hidden characteristic diagnostic features [13-17] that are difficult or impossible to see with planar imaging methods.

MRI, as one of coherent imaging modalities, detects signal in complex domain. MRI complex raw data can be decomposed into amplitude and phase images. The amplitude part provides intensity information. In spite of its common use in medical environment, this image has some limitations. Conversely, depending on the pulse sequence, the phase image can measure some physical quantities of interest which are useful for some MRI applications, such as, magnetic field inhomogeneities, magnetic susceptibility variations, velocity of flowing spins, and so on [18]. Figure 1 shows an example of amplitude and phase images derived from the MRI complex raw data. MRI phase image is extracted using arc tangent operator on the real and imaginary parts of the MRI complex raw data. Due to the ambiguity problem, however, the phase is border in the principal value range of [-π, π]. Any values exceed this interval will be border to produce the artificial phase jumps. It is called border phase or phase discontinuity. 2-D Phase Unborder (PU) is a computational process to reconstruct the unborder phase image from its principal value in modulo 2π. It is a powerful tool for solving phase problems. Much of the work has been done for various applications, such as MRI, astronomy, and optics. Compared to other applications, PU in MRI is considered to be less complicated, since the MRI data relatively has fewer phase wraps. In spite of this fact, PU in this field fails occasionally. Noise from MRI system, geometrical distortion, and motion artifact problems fairly disrupt the PU process. Accordingly, this is an area that could still require improvements.

Figure 1: (a) Amplitude

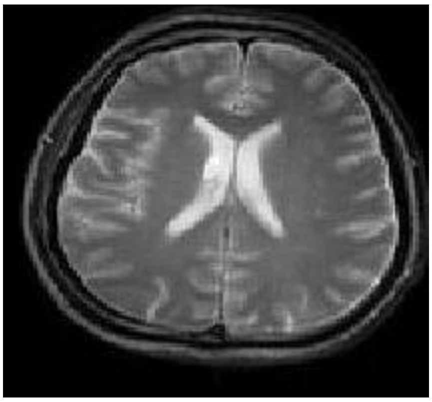

(b) Phase images of MRI complex raw data.

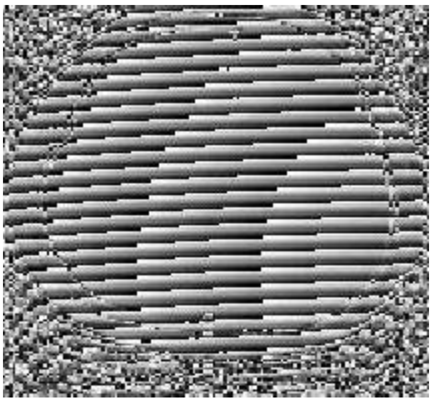

Wavelet transform is proposed to be an alternative method for MRI application. It is considered to be robust in the presence of noise with large boundary borders. Wavelet transform [19-22] is a method for complete time-frequency localization for signal analysis and characterization. Wavelet Transform works like a microscope focusing on finer time resolution as the scale becomes small to see how the impulse gets better localized at higher frequency permitting a local characterization. Wavelet Transform provides orthonormal bases while the short-term Fourier transform does not. Wavelet Transform also provides a multi-resolution signal analysis approach. Using scales and shifts of a prototype wavelet, a linear expansion of a signal is obtained. Lower frequencies, where the bandwidth is narrow (corresponding to a longer basis function) are sampled with a large time step. Higher frequencies corresponding to a short basis function are sampled with a smaller time step. Shifting and scaling of a prototype wavelet function can provide both time and frequency localization.

Reconstruction of two-dimensional (2-D) objects from their low-high frequency components has been a problem of great interest for well over a decade. Data in the form of low-high frequency components, as sample of the 2-D wavelet transform arises in several important applications. In some imaging modalities, such as MRI or Computed Tomography (CT) image transform, it is possible to sample the 2-D wavelet transform directly. In fact, in MRI, data acquisition modes corresponding to frequency samples of the 2-D wavelet transform, known as 2-D-frequency modes, may offer advantages in terms of separating frequency shift inducing phase discontinuity. In this paper, we will propose a 2-D wavelet transform with zero padding and its inverse transform for eliminating a medical phase-border image. For this reason, the paper is separately as follows. First, as above introduction, the brief review about medical image is guided. Second, the mathematical preliminaries and basic theorem for the image algorithm of wavelet transform are derived. Third, the series of image symmetrization tests based on the wavelet transform with symmetrization technique are tried. Finally, some conclusions are made and discussed.

2. Wavelet Transform for Image Processing

The wavelet transform is a method for complete frequency localization of a signal. The Fourier transform provides information about the frequency components present in the signal. However, the Fourier transform does not provide any information about frequency localization, that is, it does not provide information about when a specific frequency occurred in the signal. To improve the localization of the Fourier transform, a short-term Fourier transform can be applied. In the short-term Fourier transform method, the entire signal is split into small window and the Fourier transform is individually computed over each windowed signal. For a time-varying transforms for determining the occurrence of frequency component in specific windows. Though the short-term Fourier transform provides some localization depending on the size of the window, it does not provide complete time-frequency localization. For application in image processing and analysis, frequency localization is needed to determine the spatial position of specific frequency component in the image. The wavelet transform provide a series expansion of a signal using a set of orthonormal basis functions that are generated by scaling and translation of the mother wavelet $\Psi(t)$, and the scaling function $\Phi(t)$. The wavelet transform decomposes the signal as a linear combination of weighted basis functions to provide frequency localization with respect to the sampling parameter such as time or space. The multi-resolution approach of the wavelet transform establishes a basic framework of the localization and representation of different frequencies at different scales. If the sampling parameter is assumed to be time, a scaling function $\Phi(t)$ in time t can be defined as

$$\phi_{j,k}(t) = 2^{j/2}\phi\left(2^j t - k\right), \tag{1}$$

Where j is a scaling parameter and k is a translation parameter and j, k ∈ Z, set of all integers. The scaling and k is translation generates a family of functions using the following dilation equations

$$\phi(t) = \sqrt{2}\sum_{n=Z} h_n \phi(2t-n), \tag{2}$$

Where h_n is a set of filter (generally called low-pass filter) coefficients.

To induce a multi-resolution analysis of L^2 (R), where R is the space of all real numbers, it is required to have a nested chain of closed subspaces defined as

$$\ldots \subset V_{-1} \subset V_0 \subset V_1 \subset V_2 \subset \ldots \subset L^2 \tag{3}$$

Let us define a function $\Psi(t)$ as the "mother wavelet" such that its translated and dilated versions form an orthonormal basis of L^2 (R) to be expressed as

$$\psi_{j,k}(t) = 2^{j/2}\psi\left(2^j t - k\right) \tag{4}$$

The wavelet basis induces an orthogonal decomposition of L^2 (R), that is, one can write

$$\ldots \subset W_{-1} \subset W_0 \subset W_1 \subset W_2 \subset \ldots \subset L^2 \tag{5}$$

Where W_j is a subspace spanned by $\Psi(2^j t - k)$ for all integers j, k ∈ Z.

This basis requirement of multi-resolution analysis is satisfied by nesting of the spanned subspace similar to scaling functions, that is, $\Psi(t)$ can be expressed as a weighted sum of the shifted $\Psi(2)$ as

$$\psi(t) = \sqrt{2}\sum_n g_n \psi(2t-n), \tag{6}$$

Where g_n is a set of filter (generally called high-pass filter) coefficients. The wavelet-spanned subspace is such that it satisfies the relation

$$V_{m+1} = V_m \oplus W_m \tag{7}$$

Where $L^2 = \ldots \oplus W_{-2} \oplus W_{-1} \oplus W_0 \oplus W_1 \oplus W_2 \oplus \ldots$

Thus the wavelet functions with dilations and translations form an orthonormal basis of L^2 (**R**). Since, the wavelet function span the orthogonal complement spaces ($W_{-1} \perp W_{-2} \perp W_{-3} \perp W_{-1}$), the orthogonality requires the scaling and wavelet filter coefficient to be related through the following:

$$g_n = (-1)^n h_{1-n} \tag{8}$$

Let x[n] be an arbitrary square summable sequence representing a signal in the time domain such that

$$x[n] \in l_2(Z) \tag{9}$$

The series expansion of a discrete signal x[n] using a set of orthonormal basis function $\varphi_k[n]$ is given by

$$x[n]=\sum_{k\in Z}\langle\varphi_k(l),x(l)\rangle\varphi_k[n]=\sum_{k\in Z}X[k]\varphi_k[n] \qquad (10)$$

Where X[k]= $\langle\varphi_k(l),x(l)\rangle=\sum_l\varphi_k^*(l)x[l]$, where X[k] is the transform of x[n]. All basis functions must satisfy the orthonormality condition, that is

$$\langle\varphi_k(l),\varphi_l(l)\rangle=\delta[k-1] \qquad (11)$$

with $\|x\|^2=\|X\|^2$, where $\langle\ \rangle$ represents the inner product.

The series expansion is considered to be complete if every signal from $l_2(\mathbf{Z})$ can be expressed using the the expression in Equation (10). Similarly, using a set of bi-orthogonal basis function, the series expansion of signal x[n] can be expressed as

$$x[n]=\sum_{k\in Z}\langle\varphi_k(l),x(l)\rangle\tilde{\varphi}_k[n]=\sum_{k\in Z}\tilde{X}[k]\tilde{\varphi}_k[n]=\sum_{k\in Z}\langle\tilde{\varphi}_k(l),x(l)\rangle\varphi_k[n]=\sum_{k\in Z}X[k]\varphi_k[n]$$

,(12)

Where $\tilde{X}[k]=\langle\varphi_k(l),x(l)\rangle$ and $X[k]=\langle\tilde{\varphi}_k(l),x(l)\rangle$, and $\langle\varphi_k[n],\tilde{\varphi}_l[n]\rangle=\delta[k-1]$.

Using a quadrature-mirror filter theory, the orthonormal bases $\varphi_k[n]$ can be expressed as low-pass and high-pass filters for decomposition and reconstruction of a signal. It can be shown that a discrete signal x[n] can be decomposed into X[k] as

$$x[n]=\sum_{k\in Z}\langle\varphi_k(l),x(l)\rangle\varphi_k[n]=\sum_{k\in Z}X[k]\varphi_k[n] \qquad (13)$$

Where

$$\varphi_{2k}[n]=h_0[2k-n]=g_0[n-2k]$$
$$\varphi_{2k+1}[n]=h_1[2k-n]=g_1[n-2k]$$

And

$$X[2k]=\langle h_0[2k-l],x[l]\rangle$$
$$X[2k+1]=\langle h_1[2k-1],x[l]\rangle.$$

h_0 and h_1 are, respectively, the low-pass and high-pass filters for signal decomposition or analysis, and g_0 and g_1 are, respectively, the low-pass and high-pass filter for signal can be obtained if the orthonormal bases are used in decomposition and reconstruction stages as

$$x[n]=\sum_{k\in Z}X[2k]\varphi_{2k}[n]+\sum_{k\in Z}X[2k+1]\varphi_{2K+1}[n]$$
$$=\sum_{k\in Z}X[2k]g_0[n-2k]+\sum_{k\in Z}X[2k+1]g_t[n-2k] \qquad (14)$$

As described above, the scaling function provides low-pass filter coefficient and the wavelet function provides the high-pass filter coefficient. A muti-resolution signal representation can be constructed based on the differences of information available at two successive resolution 2^j and 2^{j-1}. Such a representation can be computed by decomposing a signal using the scaling function, a low-pass filter. The filtered signal is then sub sampled by keeping one out of every two samples. The result of low-pass filtering and sub sampling is called the scale information. If the signal has the resolution 2^j, the scale information provides the reduced resolution 2^{j-1}. The difference of information between resolution 2^j and 2^{j-1} is called the "detail" signal at resolution 2^j. The detail signal is obtained by filtering the signal with the wavelet, a high-pass filter, and sub sampling by a factor of two. Figure 2 shows wavelet based decomposition of a signal x[n] using a low-pass filter h_0 [k] (obtained from the scaling function) and a high-pass filter h_1 [k] (obtained from the wavelet function). The signal decomposition at the jth stage can thus be generalized as

$$x[n]=\sum_{j=1}^{J}\sum_{k\in Z}X^{(j)}[2k+1]g_1^{(j)}[n-2^jk]+\sum_{k\in Z}X^{(j)}[2k]g_0^{(j)}[n-2^jk]$$
$$X^{(j)}[2k]=\langle h_0^{(j)}[2^jk-l],x[l]\rangle$$
$$X^{(j)}[2k+1]=\langle h_1^{(j)}[2^jk-1],x[l]\rangle$$

(15)

In order to decompose an image, the above method for 1-D signal is applied first along the rows of the image, and then along the columns. The image, at resolution 2^{j+1}, represented by A_{j+1}, is first low-pass and high-pass filtered along the rows (Figure 2). The result of each filtering process is subsampled. Next, the subsampled results are low-pass and high-pass filtered along each column. The results of these filtering processes are again subsampled. The combination of six filtering and subsampling processes essentially provides the bandpass information. The frequency band denoted by A_j in Figure 3 is referred to as the low-low frequency band. It

Citation: Li-Hong Juang (2015), Phase Border Removing of MRI Brain Image by Wavelet Transform with Symmetrization Technique. J Mech Auto Eng 1:103

referred to as low-high, high-low, and high-high frequency band, respectively. The scheme can be iteratively applied to an image to further decompose the signal into narrower band, that is, each frequency band can be further decomposed into four narrower bands. Since each level of decomposition resolution by a factor of two, the length of the filter limits the number of levels of decomposition.

Figure 2: (a) A multi-resolution signal decomposition using wavelet transform

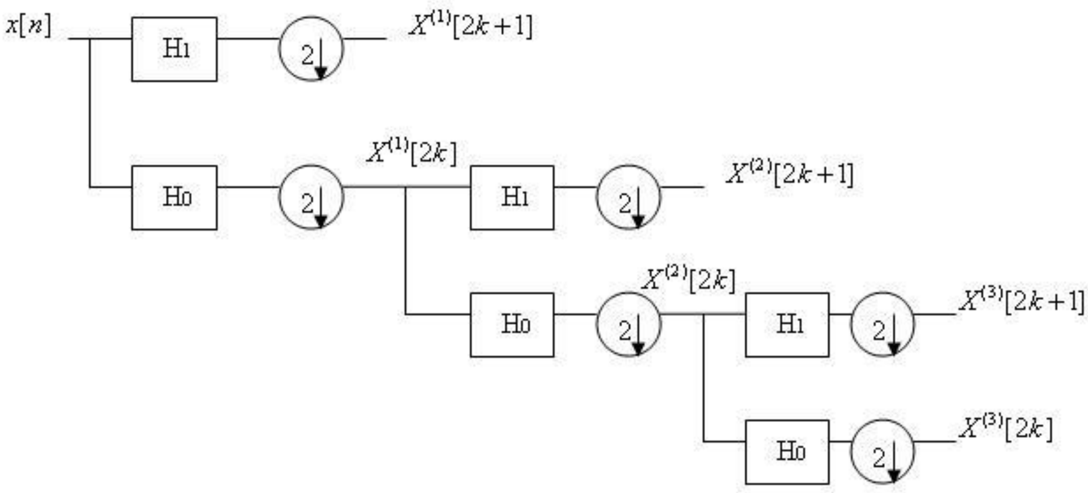

(b) The reconstruction of the signal from wavelet transforms coefficients.

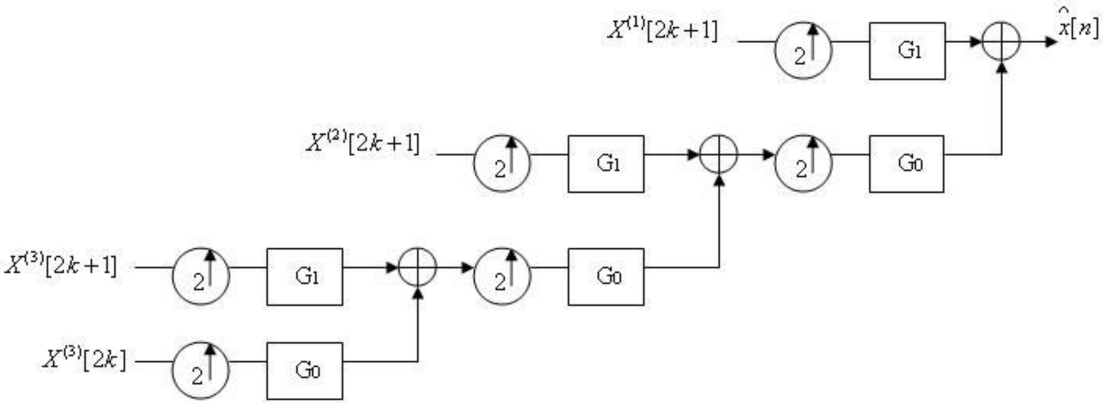

Figure 3: Multi-resolution decomposition of an image using the wavelet transform.

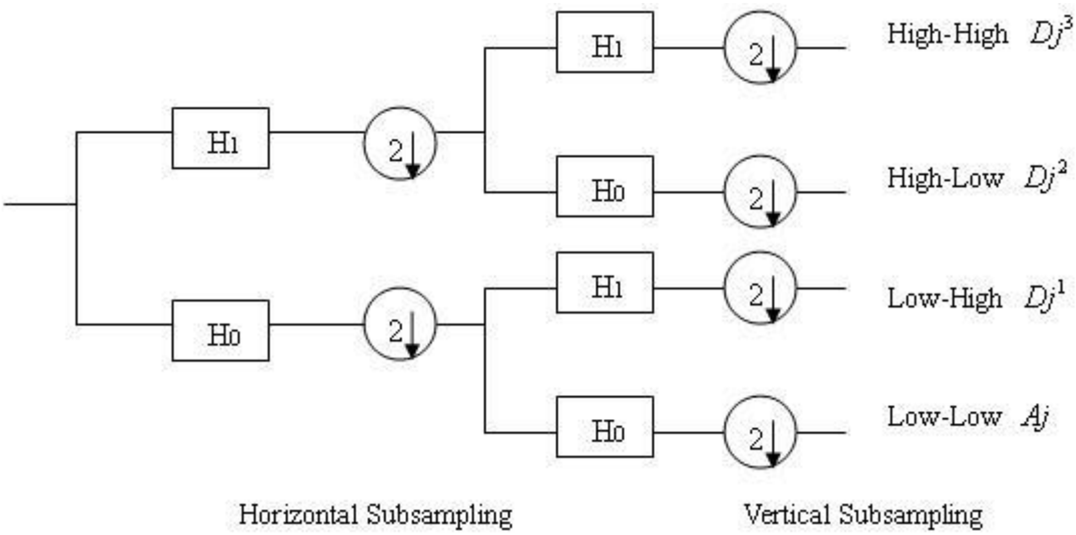

3. Simulations

The wavelet transform provides a set coefficient representing the localized information in a number of frequency bands. A popular method for denoising and smoothing is to threshold these coefficients in those bands that have a high probability of noise and then reconstruct the image using the reconstruction filters. The reconstruction filters, as described in Equation (14), can be derived from the decomposition filters using the quadrature mirror theory [19-22]. The reconstruction process integrates information from specific bands with successive up scaling of resolution to provide the final reconstructed image at the same resolution as of the input image. Symmetrization method assumes that signals or images can be recovered outside their original support by symmetric boundary value replication. It is the default mode of the wavelet transform in the signal process. Symmetrization has the disadvantage of artificially creating discontinuities of the first derivative at the border, but this method works well in general for images. Symmetrization scheme usually needs to set the extension mode and perform a decomposition of the image to defined level and symmetric wavelet number. Figure 4(a-h) shows a serial symmetrization process of the MR brain phase image using (1, 1), (2, 1), (3, 1), (4, 1), (5, 1), (6, 1), (7, 1) and (8, 1), where (L, N), L is level number and N is symmetric wavelet number. Figure 5 shows a symmetrization image using (8, 2). These results show that the optimal level and symmetric wavelet number for phase unborder is (8, 1).

Figure 4: A serial symmetrization process of the MR brain phase image using (a) (1, 1)

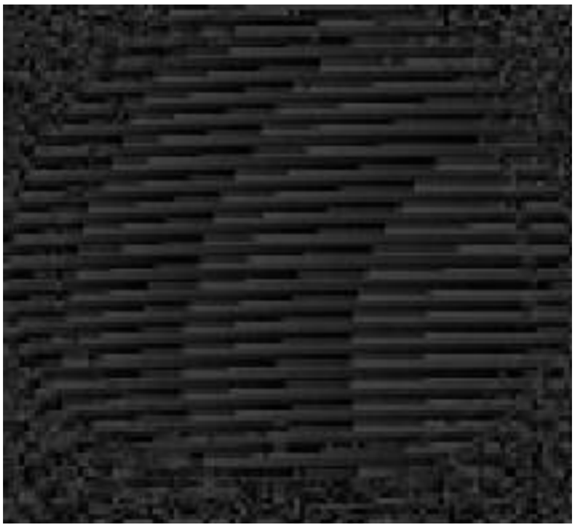

(b) (2, 1)

(c) (3, 1)

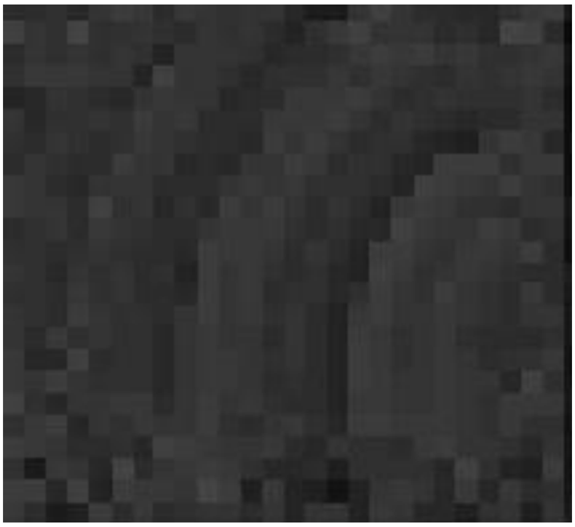

(d) (4, 1)

(e) (5, 1)

(f) (6, 1)

(g) (7, 1)

(h) (8, 1)

Figure 5: A symmetrization process of the MR brain phase image using (8, 2).

The quality of the reconstructed image depends heavily on the number of level and symmetric wavelet. For better unborder image to be reconstructed, it is essential to acquire a larger number of levels covering the entire range of boundary components around the object but a larger number of symmetric wavelets may not be necessary.

4. Conclusions

We have proposed a design and realization of phase unborder method of MRI phase images in phase border using wavelet transform with symmetrization technique. A preliminary evaluation on simulated data as well as MRI complex raw data shows encouraging results. Wavelet transform with symmetrization algorithm for phase unborder is performed to be very promising for MRI applications. The optimal level and symmetric wavelet number give significant improvements in the performance of the estimated phase border.

Acknowledgement

The authors deeply acknowledge the financial support from HuaQiao University, Fujian, P.R. China under the HuaQiao Scientific Research Foundation for Talents plan.

References

1. Rangarajan A., Hsiao I.T., Gindi G., "A Bayesian joint mixture framework for the integration of anatomical in functional image reconstruction", J Math Imaging Vision, Volume: 12, (2000), pp. 199-217.
2. Enzinger F.M., Weiss S.W., Malignant vascular tumors, Enzinger F.M., Weiss S.W., (Ed.) Soft tissue tumors, 3rd ed (1995), Mosby, St Louis, MO. pp. 655—677.
3. Hauwe L.V.D., Ramon F., Lymphatic tumors, De Schepper A.M., (Ed.) Imaging of soft tumors, 2nd ed (2001), Springer, Heidelberg. pp. 246—254.
4. Tu K.Y., Chen T.B., Lu H.H.S., Liu R.S., Chen K.L., Chen C.M., Chen J.C., "Empirical studies of cross-reference maximum likelihood estimate reconstruction for positron emission tomography", Biomed. Eng.—Appl Basis Commun, Volume: 13, Issue: 1 (2001), pp. 1-7.
5. Kao C.M., Pan X., Chen C.T., Wong W.H., "Image restoration and reconstruction with a Bayesian approach", Med Phys, Volume: 25, Issue: 5 (1998), pp. 600-613.
6. Hounsfield G. N., “Computerized transverse axial scanning tomography: Part 1, Description of the system”, Br. J. Radiol., Volume: 46, (1973), pp. 1016-1022.
7. Lipinski B., Herzog H., Kops E.R., Oberschelp W., Muller-Gartner H.W., "Expectation maximization reconstruction of positron emission tomography images using anatomical magnetic resonance information", IEEE Trans Med Imaging, Volume: 16, Issue: 2 (1997), pp. 129-136.
8. Bazille A., Guttman M.A., Mcveigh E.R., Zerhouni E.A., “Impact of semiautomated versus manual image segmentation errors on myocardial strain calculation by magnetic resonance tagging”, Invest Radiol, Volume: 29, Issue: 4 (1994), pp. 427—433.
9. Anger, H., “Use of gamma-ray pinhole camera for vivo studies”, Nature, Volume: 170 (1952), pp. 200-204.
10. Ouyang X., Wang W.H., Johnson V.E., Hu X., Chen C.T., "Incorporation of correlated structural images in PET image reconstruction", IEEE Trans Med Imaging, Volume: 13, Issue: 2 (1994), pp. 627-640.
11. Akgul YS, Kambhamettu C, Stone M. Extraction and tracking of the tongue surface from ultrasound image sequences. In: Proceedings IEEE computer vision pattern recognition, Santa Barbara, CA; (1998). p. 298–303.
12. Abeyratne, U.R.; Petropulu, A.P.; Reid, J.M., "On modeling the tissue response from ultrasonic B-scan images" IEEE Trans. on Med. Imaging, Volume: 1, Issue: 2 (1996), pp. 479-490.
13. Faber, T.L., Stokely E.M., "Orientation of 3D structures in medical images", IEEE Trans. Pattern Anal. Machine Intel., Volume: 2, Issue: 2 (1980), pp. 127-135.
14. Grewera, G.J., Udupa J.K., "Shape based interpolation of multidimensional grey-level images", IEEE Trans. Medical Imaging, Volume: 15, Issue: 6 (1996), pp. 881-892.
15. Cohen, F.S.; Georgiou, G.; Halpern, E., "WOLD decomposition of the backscatter echo in ultrasound images of soft tissue organs" IEEE Trans. Ultrason., Ferroelect. Freq. Contr., Volume: 1, Issue: 2 (1997), pp. 460-472.
16. Donohue, K.D.; Forsberg, F.; Piccoli, C.W.; Goldberg, B.B., "Classification of breast masses with ultrasonic scattering structure templates" IEEE Trans. Ultrason., Ferroelect. Freq. Contr., Volume: 1, Issue: 2 (1999), pp. 300-310.
17. Georgiou, G.; Cohen, F.S., "Statistical characterization of diffuse scattering in ultrasound images" IEEE Trans. Ultrason., Ferroelect. Freq. Contr. (1998), pp. 57-64.
18. Liang, Z. P., “A model-based method for phase unwrapping”, IEEE Trans., Medical Imaging, Volume 15, Issue: 6 (1996), pp. 300-310.
19. Daubechies, I., “Ten lectures on Wavelets”, Society for Applied Mathematics (1992), Philadelphia.
20. Coifman, R.R.; M.V Wickerhauser, "Entropy-based algorithms for best basis selection," IEEE Trans. on Inf. Theory, Volume 38, Issue: 2 (1992), pp. 713-718.
21. DeVore, R.A.; B. Jawerth, B.J. Lucier, "Image compression through wavelet transform coding," IEEE Trans. on Inf. Theory, Volume 38, Issue: 2, (1992), pp. 719-746.
22. Donoho, D.L., "De-Noising by soft-thresholding," IEEE Trans. on Inf. Theory, Volume 41, Issue: 3, (1995), pp. 613-627.